



**CHALMERS**  
UNIVERSITY OF TECHNOLOGY

## **High-speed low-power and board-mountable optical transceivers for scalable & energy efficient advanced on-board digital processors**

Downloaded from: <https://research.chalmers.se>, 2026-04-04 00:03 UTC

Citation for the original published paper (version of record):

Stampoulidis, L., Kehayas, E., Karppinen, M. et al (2018). High-speed low-power and board-mountable optical transceivers for scalable & energy efficient advanced on-board digital processors. Proceedings of SPIE - The International Society for Optical Engineering, 11180. <http://dx.doi.org/10.1117/12.2536075>

N.B. When citing this work, cite the original published paper.

# International Conference on Space Optics—ICSO 2018

Chania, Greece

9–12 October 2018

*Edited by Zoran Sodnik, Nikos Karafolas, and Bruno Cugny*



## ***High-speed low-power and board-mountable optical transceivers for scalable & energy efficient advanced on-board digital processors***

*L. Stampoulidis*

*E. Kehayas*

*M. Karppinen*

*A. Tanskanen*

*et al.*



International Conference on Space Optics — ICSO 2018, edited by Zoran Sodnik, Nikos Karafolas, Bruno Cugny, Proc. of SPIE Vol. 11180, 111804C · © 2018 ESA and CNES · CCC code: 0277-786X/18/\$18 · doi: 10.1117/12.2536075

Proc. of SPIE Vol. 11180 111804C-1

# High-speed, low-power and board-mountable optical transceivers for scalable & energy efficient advanced on-board digital processors

L. Stampoulidis<sup>a</sup>, E. Kehayas<sup>a</sup>, M. Karppinen<sup>b</sup>, A. Tanskanen<sup>b</sup>, J. Ollila<sup>b</sup>, J. Gustavsson<sup>c</sup>, A. Larsson<sup>c</sup>, L. Grüner-Nielsen<sup>d</sup>, Christian Larsen<sup>d</sup>, M. Sotom<sup>e</sup>, Anaëlle Maho<sup>e</sup>, Mickael Faugeron<sup>e</sup>, N. Venet<sup>e</sup>, M. Ko<sup>f</sup>, P. Ostrovskyy<sup>f</sup>, D. Kissinger<sup>f</sup>, R. Safaisini<sup>g</sup>, R. King<sup>g</sup>, I. McKenzie<sup>h</sup>, J. B. Gonzalez<sup>i</sup>

<sup>a</sup>Gooch&Housego, <sup>b</sup>VTT Technical Research Centre of Finland, <sup>c</sup>Chalmers University of Technology, <sup>d</sup>OFS Denmark, <sup>e</sup>Thales Alenia Space, <sup>f</sup>IHP GmbH Institute for Innovative Microelectronics, <sup>g</sup>Philips Photonics GmbH, <sup>h</sup>ESTEC, European Space Agency, <sup>i</sup>ALTER Technology

## ABSTRACT

We present the development and verification testing of a high speed multimode, multicore transceiver technology for intra-satellite optical interconnects. We report the fabrication and functional testing of opto-parts including 25 Gb/s 850 nm VCSEL/PD as well as the verification testing of the VCSELs against radiation and lifetime performance. In addition we report the development and evaluation testing of a multi-core cable assembly that was fabricated and mated with MiniAVIM multi-core connectors to develop hi-rel multi-core optical patchcords for pigtailling the transceiver modules. The fiber optic, electronic and opto-parts were used to assemble the first ever fully packaged and pigtailed, six-core optical transceiver prototype module that operates at 25 Gb/s channel bit rate at an energy consumption of <4.5 mW/Gb/s.

**Keywords:** Optical interconnects, optical transceiver, VCSEL, photo-detector, fiber optic cable, rad-hard digital circuits

## 1. INTRODUCTION

Multi-Gb/s optical interconnects (OI) are expected to be deployed within advanced on-board digital processor systems in the new-gen telecommunication satellites. In addition, OIs are expected to implement SpaceFibre optical links within remote sensing payloads deployed in Earth Observation missions. In these applications optical transceivers that employ multimode 850 nm VCSEL/PD technology are required to transfer data between modules and ASICs at bit rates > 10 Gb/s and at the lowest possible energy consumption.

The European ROBIN research project [1] has recently concluded the development and demonstration of a board-mountable optical transceiver designed to deliver an aggregate bit rate of 150 Gb/s (6 ch x 25 Gb/s line rate) at a per channel power consumption as low as 109.5 mW which corresponds to <4.5 mW/Gb/s energy consumption. In this paper we present the fabrication and evaluation of the ROBIN transceiver fiber optic parts including: a) 25 Gb/s multimode (MM) 850 nm VCSEL and PD arrays and b) MM, multi (6) - core (MC) fiber optic cable and mini-AVIM pigtail. We present functional and targeted environmental testing of these parts demonstrating acceptable performance over temperature, radiation, lifetime and material outgassing constraints.

In addition, we present the assembly and functional testing of the MM, MC transmitter and receiver optical sub-assemblies that consist of:

- a) Transmitter Optical Sub-assembly (TOSA): 6 channel circular 25 Gb/s VCSEL array wire bonded to a twin array of 25 Gb/s VCSEL driver ICs and
- b) Receiver Optical Sub-assembly (ROSA): 6-channel, circular 25 Gb/s PD array wire bonded to a twin array of 25 Gb/s TIA ICs.

Finally, we demonstrate the integration and packaging of a small form factor optical transceiver module prototype that consisted of the MM, MC-TOSA and ROSA devices coupled to the MiniAVIM MM, MC pigtail. The ROBIN transceiver module has been functionally tested up to 25 Gb/s within the ROBIN end-user test-bed.

# International Conference on Space Optics—ICSO 2018

Chania, Greece

9–12 October 2018

*Edited by Zoran Sodnik, Nikos Karafolas, and Bruno Cugny*



## ***High-speed low-power and board-mountable optical transceivers for scalable & energy efficient advanced on-board digital processors***

*L. Stampoulidis*

*E. Kehayas*

*M. Karppinen*

*A. Tanskanen*

*et al.*



ics0 proceedings



## 2. OPTO-PART DEMONSTRATION

### 2.1 High speed multimode, multi-core VCSEL and PD arrays

#### 2.1.1 Fabrication, functional verification and environmental test plan

VCSEL and PD arrays have been fabricated in a circular configuration to match the geometry of the multi-core fiber (MCF) that would be used for the optical transceiver pigtailing. The circular, multi-core solution was chosen in order to enable a 150 Gb/s parallel optical data link through a single optical fiber, thus minimizing the module fiber count and improving the integration density of the interconnections. As an upside benefit, the capability to mate the MCF with multi-core MiniAVIM connectors, makes the solution attractive in terms of reliability compared to COTS ribbon fiber connectors. In addition, the multi-core cable favors the manufacturability of robust hermetic fiber feedthroughs required for the module hermetic packaging/pigtailing. In a previous publication [2] we have presented robust performance of 40 Gb/s VCSEL prototypes at temperatures up to 85°C and at low bias/modulation currents by Chalmers University of Technology. Here we present the fabrication and performance of devices that have been fabricated within PHILIPS qualified manufacturing line. The fabrication transfer to PHILIPS was done in an effort to increase the device TRL level and progress the research prototype to an industrial product. The figure below (left) shows the microscope image of a 3  $\mu\text{m}$  ( $\text{Ø}22$ ) and a 5  $\mu\text{m}$  ( $\text{Ø}24$ ) aperture size circular VCSEL array. The chip size is 720 x 420  $\mu\text{m}$  (LxW). The figure below (mid and right) shows the L-I-V performance recorded at 25°C. At a bias current of 5 mA - which is within the current range provided by the BICMOS VCSEL driver IC - both VCSELs deliver >1.5 mW output power. As expected the larger diameter VCSEL exhibits a better scaling of the output power with no roll-off of the output power at currents up to 10 mA. The output power at 10 mA is 3.2 mW.

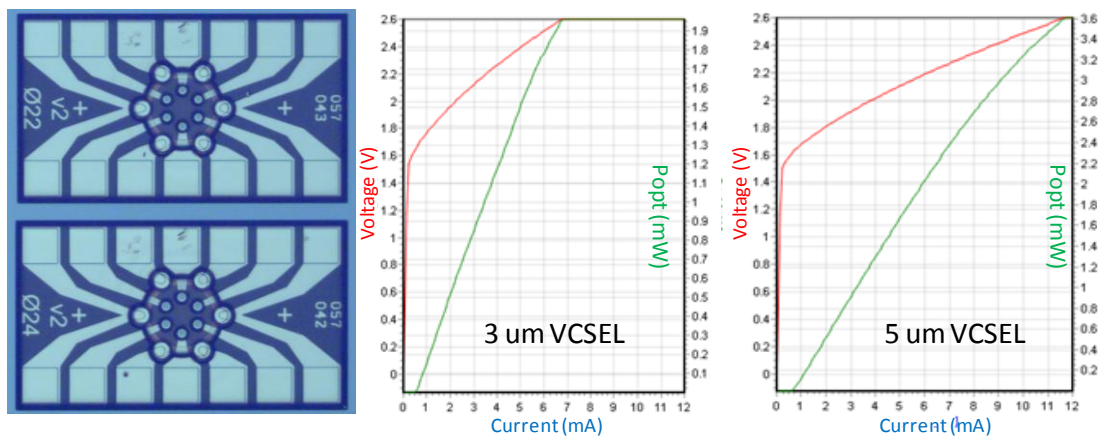


**Figure 1.** (left) Microscope image of the 6-channel VCSEL arrays and L-I-V curve of 3  $\mu\text{m}$  VCSEL array (middle) and 5  $\mu\text{m}$  VCSEL (right)

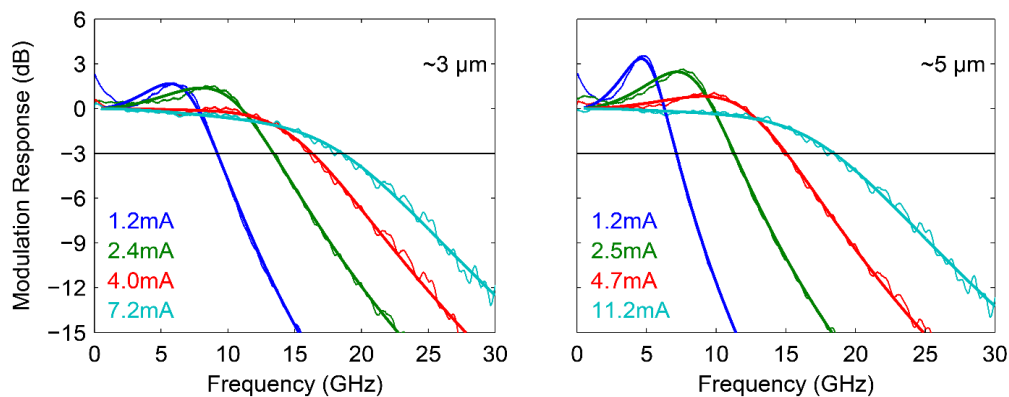


**Figure 2.** Small signal modulation response at different currents recorded at 25°C: (left) 3  $\mu\text{m}$  aperture VCSEL, (right) 5  $\mu\text{m}$  aperture VCSEL

The small signal modulation response (from S21 measurements) at different bias currents and at 25°C is shown in the figure above. The 3  $\mu\text{m}$  VCSEL demonstrates a -3dB modulation bandwidth of >17 GHz at 4 mA bias current. For the 5  $\mu\text{m}$  aperture VCSEL, at a current of 4.7 mA mA the -3dB modulation bandwidth is >15 GHz. Increasing the current to 11 mA increases the bandwidth closer to 20 GHz. Both performances are sufficient for 25 Gb/s modulation and transmission. To verify this assumption high speed modulation tests at 25 Gb/s and at various currents have been performed. The figures below illustrate the eye diagram analysis for both VCSEL arrays and at driving currents ranging from 4 mA up to 8 mA. In all cases clear eye diagrams have been obtained with extinction ratios (ER) as high as 5 dB. For the 5  $\mu\text{m}$  VCSEL the eye diagram improvement is evident as the bias current increases due to the improvement of the device modulation bandwidth.

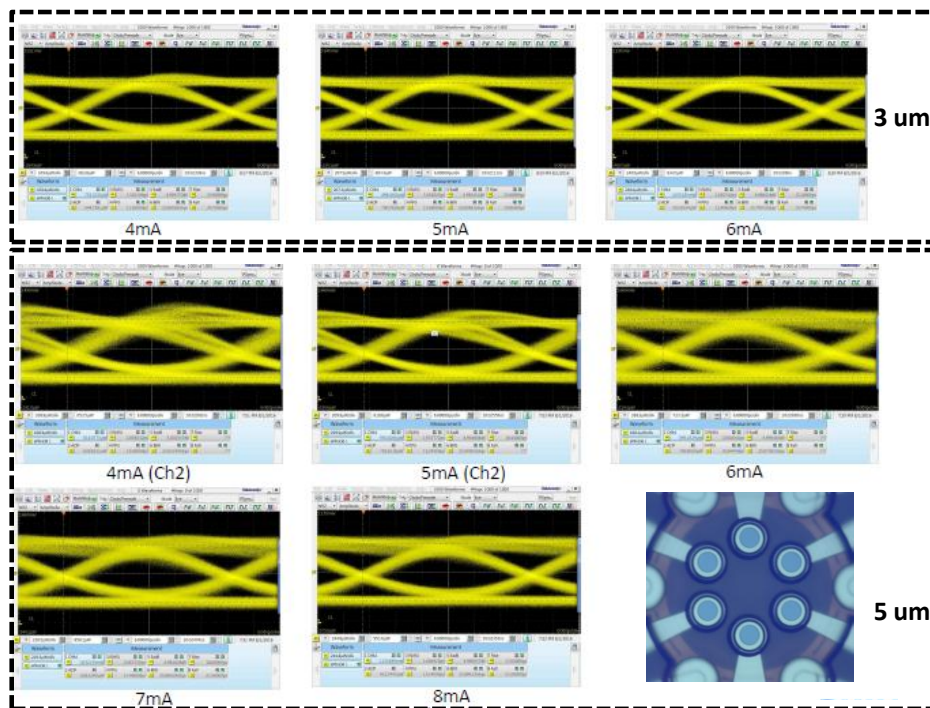


**Figure 3.** Eye diagrams of VCSEL arrays: (top) 3  $\mu\text{m}$  aperture VCSEL, (bottom) 5  $\mu\text{m}$  aperture VCSEL. Modulation speed is 25 Gb/s.

Multimode 850 nm PDs were also fabricated within PHILIPS manufacturing line. The figure below (inset) shows the microscope image of the six element circular array. Chip size is similar to the VCSEL array. The aperture of each PD is 24  $\mu\text{m}$  and was chosen as an optimum trade-off between bandwidth and coupling to the MCF cores.

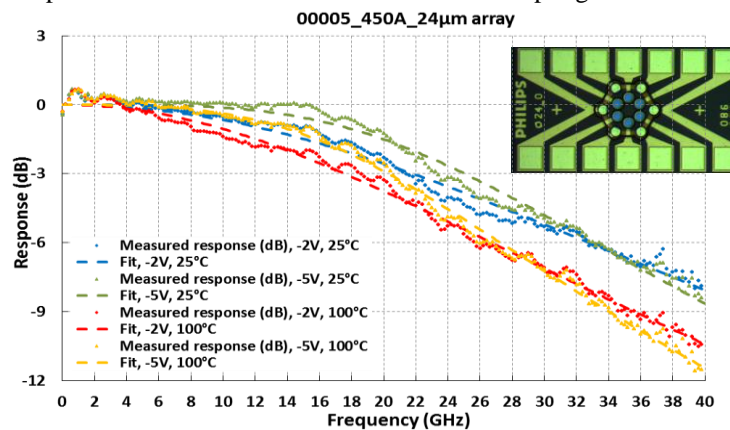


**Figure 4.** Frequency response measurements of the PD wafer at 25°C and 100°C. Dashed lines present fits to the measured data. (inset) microscope image of the PD chip

The figure above shows measured frequency responses of the PD wafer at 25°C and 100°C along with the corresponding fits after subtracting out the VCSEL response from the total PD/VCSEL response. The 3dB cut-off frequency extracted from the fits are 25 GHz and 20 GHz at 25°C and 100°C respectively and at -5V reverse bias voltage. This measurement indicates that the PD is well capable for detection of 25 Gb/s modulated signals. Concerning the device testing both VCSEL and PD chips were subjected to a radiation and lifetest. Here we focus on the tests performed on the VCSEL parts. The figure below shows the test plan that was followed for the VCSEL environmental testing. A total of 32 samples were delivered for testing; 2 samples were used as reference, 4 samples were subjected to radiation tests (2x in Gamma and 2x in proton) and 16 samples were subjected to an accelerated life test. The radiation test conditions followed ESCC 22900 and the radiation test levels are tailored to comply with typical LEO and GEO telecommunication missions. The life test followed PHILIPS internal test protocol for VCSEL wafer qualification.

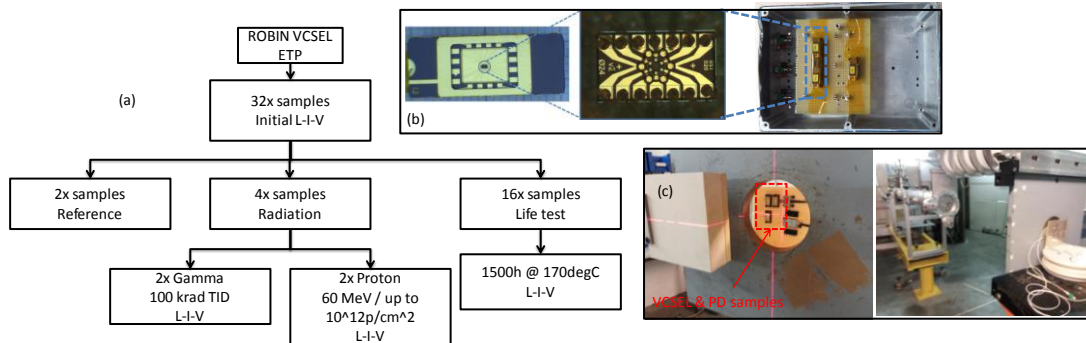


**Figure 5.** (a) VCSEL array test plan, (b) packaging and configuration of the test samples for gamma radiation test, (c) proton radiation test set-up, front view: VCSEL and PD components aligned with proton beam, rear view: samples against the proton generator

### 2.1.2 Radiation and accelerated life testing

The two VCSEL designs (3  $\mu\text{m}$  and 5  $\mu\text{m}$  aperture size) have been subjected to gamma radiation testing. The radiation facility was CNA (Centro Nacional de Aceleradores) Gamma Facility in Seville, Spain. The chips were mounted and wire-bonded into DIL package modules to enable in-situ functional testing at the different steps during irradiation as shown in figure 5b). Current was supplied to the lasers through the package pins and the optical power emitted by the VCSELs was collected through free space by integrating sphere detector for L-I-V measurements. Packaging and testing was performed by ALTER. The TID was 100 krad at a dose rate of 210 rad/h. Modules were in OFF state (unbiased) during radiation. The following graphs present the results of the L-I-V characterization of the two VCSEL types. All six VCSELs in each array have been tested - here we present L-I-V characterization for one VCSEL in each array, since all the lasers in the array responded uniformly. The driving current was tuned from 0-10 mA at steps of 0.025 mA (for 0-2.5 mA) and 0.25 mA (for 2.5-10 mA). The results validate the efficiency saturation of the 3  $\mu\text{m}$  VCSEL variant. A reference VCSEL array sample for each array under test was used at each measurement step in order to ensure measurement repeatability.

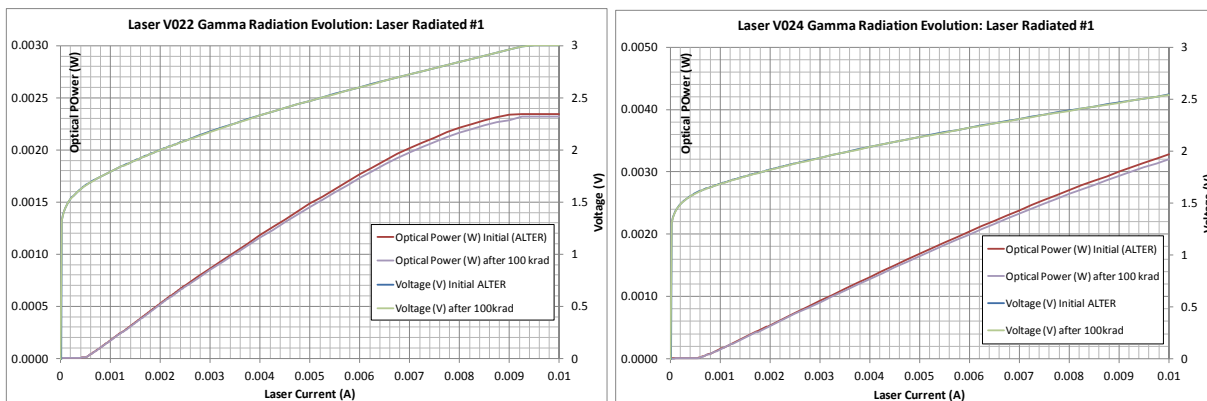


**Figure 6.** (left) VCSEL array gamma test results. L-I-V curves at 0 and 100 krad for: (left) 3  $\mu\text{m}$  aperture VCSEL, (right) 5  $\mu\text{m}$  aperture VCSEL

The prototype VCSEL arrays exhibited stable performance under gamma irradiation. The results indicate no drift of the VCSEL array laser threshold current and as such no impact on the laser efficiency at the radiation levels of interest. Measurements are in agreement with literature which suggests that displacement damage effects induced by gamma radiation would appear at much higher TID levels. In addition two similar VCSEL arrays were subjected to proton radiation testing. Proton testing was done by ALTER using UCL CYCLONE110 (CYClotron de LOuvain-la-NEuve) facility. The test conditions are outlined below.

PROTON TESTING FOR MM-MC VCSEL				
STEP	60Mev Beam flux (cm <sup>-2</sup> s <sup>-1</sup> )	Beam time (s)	Accumulated beam time (s)	Cumulative fluence
1	1 · 10 <sup>8</sup>	100s	100s	1 · 10 <sup>10</sup>
2	1 · 10 <sup>8</sup>	900s	1000s	1 · 10 <sup>11</sup>
3	1 · 10 <sup>8</sup>	8900s	10000s	1 · 10 <sup>12</sup>

Table 1. proton radiation test condition

The figure below shows the L-I-V test results recorded at the three steps. Similar to the gamma radiation tests, the L-I-V curves show no drift of the laser threshold current and as such no impact of the laser efficiency at a cumulative fluence up to 10<sup>12</sup> p/cm<sup>2</sup>.

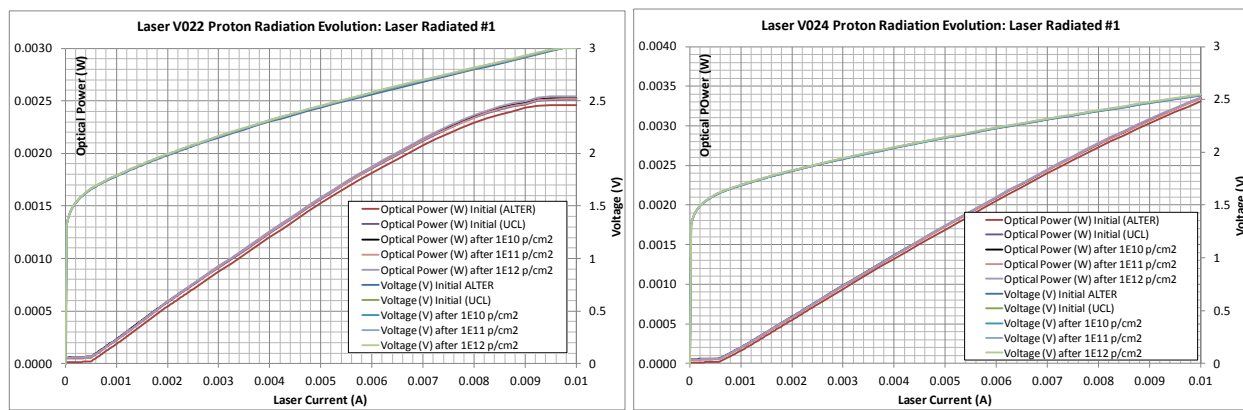


Figure 7. (left) VCSEL array proton test results. L-IV curves at the three steps for: (left) 3 um aperture VCSEL, (right) 5 um aperture VCSEL

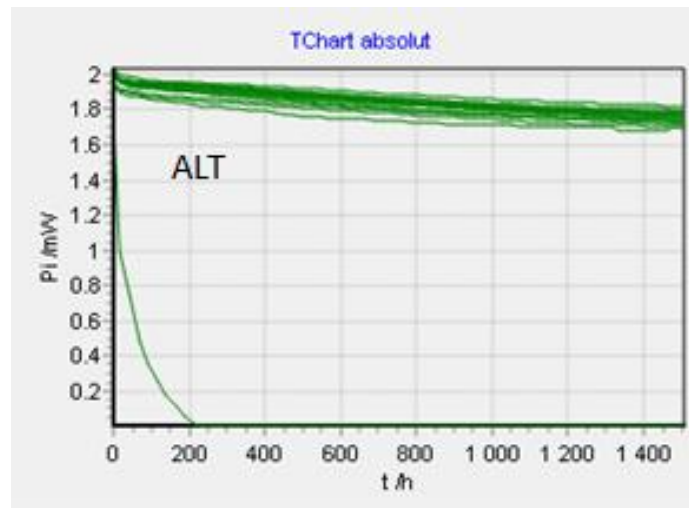


Figure 8: VCSEL array ALT test result

Finally, 16 VCSEL samples were subjected to an accelerated life test 1500 h biased at 6 mA at a temperature of 170°C. The samples were selected randomly from the produced VCSEL batch and there was no screening applied following the part selection. The pass/fail criterion was a power drop of <2dB which corresponds to a MTTF>1000hrs. The figure above shows the evolution of the output power emitted by the VCSEL samples during the 1500h lifetest. There was an early failure observed on a channel whereas the other 15 channels operated normally and with no failure up to 1500h. The failure within the first hours of the test would have been captured by standard screening which foresees an 168 h burn-in to detect samples with infant mortality.

### 2.2 Multimode, Multi-core rad-hard fiber optic patchcord

A multimode, multi-core fiber sample was fabricated by OFS - the fiber was developed to couple light in/out of the multi-element VCSEL/PD arrays. As such the core arrangement (shown in figure 9 (a)) matched the geometry of the opto-chips and the graded-index core composition was adapted to achieve enhanced radiation tolerance. A cable assembly was fabricated using the multi-core fiber and the OFS  $\mu$ linx® cable.



**Figure 9:** a) Profile of multi-mode, multi-core fiber, b) cable sample connected to fan-outs for radiation testing, c) end-face of multi-core MiniAVIM connector and d) assembled multi-core, MiniAVIM patchcord prototype

The  $\mu$ linx® cable deploys a high temperature ETFE outer jacket with a diameter of 0.8 mm which supports a long term bending radius as low as 8 mm and exhibits a wide operating temperature range of -40 to +100 °C. Following production, a 650 meter and a 500 meter sample were characterized for attenuation using the OTDR method. The average attenuation for the six cores was 2.45 and 2.56 dB/km for the two samples which compare very well with the 2.3 dB/km and 2.1 dB/km found in commercial single core radiation hard fibers and commercial standard multimode fibers respectively. The performance of the  $\mu$ linx® cable assembly was characterized against material outgassing. The test followed the ECSS-Q-ST-70-02C standard for thermal vacuum outgassing test for the screening of space materials and was conducted at Aerospace & Advanced Composites GmbH in Vienna. The pass/fail criterion is a CVCM and RML <1%. Four samples were subjected to the mass loss test; three of them were subjected to a pre-annealing process to enhance outgassing performance and one of them was a pristine sample.

Material	TML		RML		WVR		CVCM		Acceptance limits achieved:
	Mean	StdDev	Mean	StdDev	Mean	StdDev	Mean	StdDev	
	[%]	[%]	[%]	[%]	[%]	[%]	[%]	[%]	
Intrinsic	<b>0.86</b>	0.01	<b>0.60</b>	0.01	<b>0.26</b>	0.00	<b>0.03</b>	0.02	<b>YES</b>
Annealed 1 h @ 125°C	<b>0.76</b>	0.01	<b>0.52</b>	0.02	<b>0.25</b>	0.01	<b>0.03</b>	0.01	<b>YES</b>
Annealed 1h @ 150°C	<b>0.73</b>	0.01	<b>0.48</b>	0.01	<b>0.25</b>	0.00	<b>0.01</b>	0.00	<b>YES</b>
Annealed 24h @ 125°C	<b>0.72</b>	0.00	<b>0.47</b>	0.02	<b>0.25</b>	0.02	<b>0.02</b>	0.00	<b>YES</b>

Table 2. Result from Vacuum mass loss test according to ECSS-Q-ST-70-02C

The mass loss test results are shown in table 2; even the intrinsic sample passed the test exhibiting an RML<0.6% and a CVCM as low as 0.03%. Still the annealing even further improves the result. Figure 9 (b) shows the sample that was

subjected to the gamma radiation test in order to characterize the cable assembly in terms of radiation induced absorption (RIA). The sample consisted of 100 meters of multi-core cable that was spliced to two multi-core to single-core fan-outs. The fan-out devices were used to launch and collect light through standard single core fiber interfaces and were kept outside of the radiation area. The test was performed by ALTER using the same Cobalt source as with the VCSEL test described above. The TID was 104.5 krad and the dose rate was 218 rad/h. A 850 nm laser source and detector were used to characterize the loss of the cable sample. The following graph shows the evolution of the relative optical power measured at the fan-out port. The forward voltage and the internal photodiode current on the laser have been monitored to ensure that the laser is working properly during test.

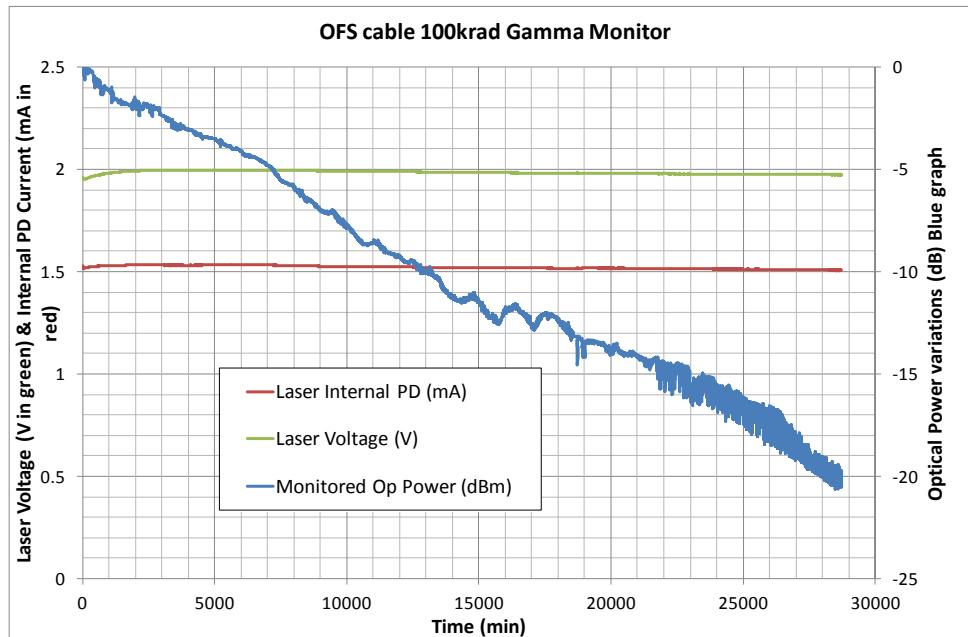


Figure 10: MM-MC cable assembly gamma irradiation test results

The evolution of the optical power shows a linear drop during the test, which is evidence of radiation hard performance. A total of 20 dB loss is recorded at the end of the test. Considering that the irradiated cable coil had a length of 100 m this leads to the following result:

- Optical attenuation at 104.5 krad TID at 850 nm: 0.2 dB/m
- Optical attenuation per meter and krad: 0.0019 dB/m/krad

The connector of choice for the multi-core rad-hard cable was the MiniAVIM connector commercialized by Swiss DIAMOND. The MiniAVIM was selected since it is the first space qualified optical connector part as per ESCC standards. In addition, the MiniAVIM connector exhibits a low mass (1.12 grams) and as such the multi-core pigtails will not add significant mass to the total mass of the transceiver module. Figure 5c) shows the end-face of the MiniAVIM connector which was developed by precision drilling of a circular arrangement of holes to support the multi-core fiber. Figure 5d) show a multi-core MiniAVIM patchcord prototype. The patchcord was characterized in terms of insertion loss and crosstalk. Two fan-outs have been used to launch light into and collect light from each one of the six cores of a patchcord. The fan-outs have been characterized in terms of insertion loss and their losses have been subtracted from the insertion loss measurement of the patchcords. The table below shows the obtained insertion loss and crosstalk test results for 12x multi-core MiniAVIM patchcords. The insertion loss is quite stable with only 0.15 dB standard deviation, with min and max values being 0.95 and 1.54 dB respectively (average of 1.19 dB). The cross-talk has been measured around 15.8 dB. The high cross talk (low core to core isolation) is attributed to the quality of the fan-outs and not the connectors.

S/N <sub>j</sub> - Core/N→	Insertion Loss, IL [dB]						Cross talk	
	1	2	3	4	5	6	CT	channels
2113615.001	0.98	1.12	1.05	1.20	1.05	1.18	15.73	FA1-1 to FA2-2
2113615.002	1.04	1.48	1.45	1.53	1.42	1.2		
2113615.003	1.11	1.20	1.40	1.20	1.21	1.11	15.71	FA1-1 to FA2-2
2113615.004	1.09	1.12	1.20	1.07	1.2	1.13		
2113615.005	1.04	1.29	1.25	1.38	1.23	1.12	15.94	FA1-1 to FA2-2
2113615.006	1.14	1.38	1.29	1.54	1.33	1.34		
2113615.007	1.01	0.95	0.96	1.07	1.13	1.03	15.88	FA1-1 to FA2-2
2113615.008	1.07	1.13	1.29	1.27	1.19	1.16		
2113615.009	1.16	1.04	1.14	1.21	1.29	1.09	15.83	FA1-1 to FA2-2
2113615.010	1.17	1.18	1.18	1.25	1.16	1.09		
2113615.011	0.99	1.21	1.14	1.48	1.18	1.24	15.49	FA1-1 to FA2-2
2113615.012	1.01	1.36	1.11	1.22	1.04	1.08		

Table 3: Measured insertion loss and crosstalk of 12x multi-core, MiniAVIM patchcords

### 3. TRANCEIVER MODULE DEMONSTRATION

High speed multi-core VCSELs have been assembled together with high speed VCSEL driver array ICs into a TOSA module as shown in the figure below. The lasers in the circular array were wire bonded to two driver IC chips that were placed on the opposite sides of the VCSEL array. In order to obtain a good signal integrity at 25 Gbps/channel the wire bond lengths were minimized, a high-speed substrate material was used and careful matching of the transmission lines was implemented. The ROSA followed the same assembly concept and integrated a circular PD array and TIA ICs.

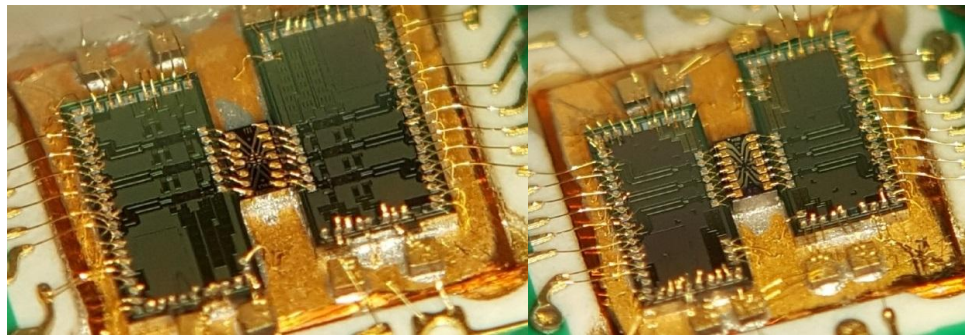


Figure 11: Micrographs of TOSA (right) and ROSA (left) optical subassemblies

The driver and TIA ICs were developed by IHP and were equipped with a SPI-standard digital serial interface in order to enable advanced digital control functions. The driver IC provides channel-independent digital control of channel on/off, VCSEL bias/modulation currents, and pre-emphasis level. It is also available to monitor the VCSEL diagnostic information via SPI. Similarly, the TIA IC provides control of channel on/off, jitter (noise) optimization, gain, and output amplitude. The total power consumption for a transceiver channel is shown below.

	Measured Tx	Measured Rx	Measured Total	Target Total
Consumption/channel ON	42.5	67.1	109.6	< 120
Consumption/channel OFF	0.9	4.2	5.1	< 10

Table 4 Total power consumption of transceiver module electronics (VCSEL driver IC and TIA IC)

Measurements show a power consumption per channel of 109.6 mW which corresponds to a 4.38 mW/Gb/s power consumption. The figure below shows the prototype multi-core transceiver module assembled by VTT mounted on an evaluation board. The device brings together the TOSA and ROSA chipsets with the VCSEL and PD arrays coupled to two multi-core MiniAVIM pigtailed. The inset shows a clear 10 Gb/s eye diagram obtained when the transmitter and receiver were connected in a loop-back configuration.

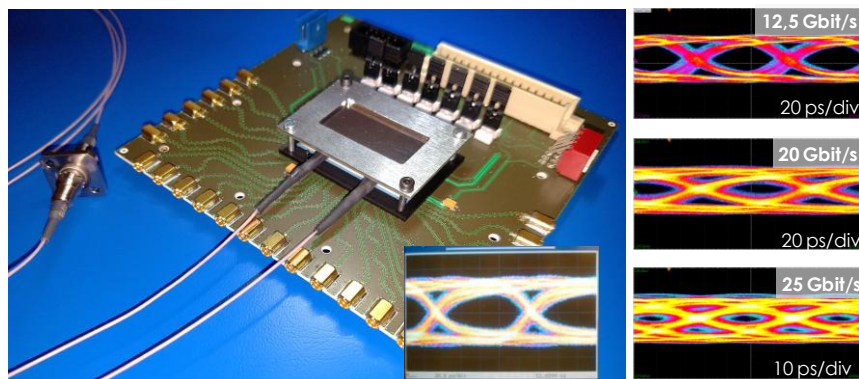


**Figure 12:** (left) Prototype multi-core transceiver module, (inset) 10 Gb/s eye diagram in back-to-back configuration, (right) eye diagrams at 12.5, 20 and 25 Gb/s when connecting the TOSA and ROSA devices through fan-outs

The transceiver module was evaluated in a transmission test-bed assembled by Thales Alenia Space (Toulouse). The test configuration included fan-out devices connected to the output of the multi-core transmitter and the input of the multi-core receiver. Figure 12 (right) shows the eye diagrams obtained at 12.5 Gb/s, 20 Gb/s and 25 Gb/s respectively. Regarding BER performance, error free operation was achieved at 17.5 Gb/s whereas a BER of  $10^{-9}$  was obtained at 20 Gb/s.

#### 4. CONCLUSION

We have demonstrated the development of the first fully packaged and pigtailed multi-core transceiver module operating at bit rates beyond 10 Gb/s. We have reported the fabrication, functional testing and environmental evaluation testing of the key opto-parts including the VCSEL arrays, PD arrays and fiber optic cable. In most development areas the technology has proven robust operation and as such is now ready for further exploitation towards the development of robust, radiation hard space transceiver modules.

#### 5. ACKNOWLEDGEMENT

The authors would like to thank Frederic Taugwalder from DIAMOND for fruitful technical discussions on the feasibility of multi-core fiber optic connector assemblies. DIAMOND is acknowledged for delivering the multi-core MiniAVIM connector parts.

#### 6. REFERENCES

- [1] [www.space-robin.eu/](http://www.space-robin.eu/)
- [2] A. Larsson, et. al, "VCSEL design and integration for high-capacity optical interconnects", (invited paper) in Proc. SPIE 10109, Optical Interconnects XVII, 101090M, Optical Interconnects XVII, in SPIE Photonics West Conference 2016, San Francisco, California, United States, 15-17 February 2017